Thermal Analysis of Workpiece under Electrical Discharge Machining (EDM), Using Hyperbolic Heat Conduction Model

Seyfolah Saedodin
Department of Mechanical Engineering,
Islamic Azad University, Semnan Branch, Semnan, Iran
E-mail: S_Sadodin@iust.ac.ir

Mohsen Torabi*
Department of Mechanical Engineering,
Semnan University, Semnan, Iran
E-mail: Torabi_mech@yahoo.com
*Corresponding author

Hadi Eskandar
Department of Mechanical Engineering,
Semnan University, Semnan, Iran
E-mail: Hadi.Eskandar@gmail.com

Received 4 May 2010; Revised 29 July 2010; Accepted 11 September 2010

Abstract: Whereas in electrical discharge machining (EDM) the heat flux entering the workpiece is extremely high, the Fourier heat conduction model may fails. This article reports on determination of temperature distribution in the workpiece due to EDM using non-Fourier heat conduction model. Equations are solved by deriving the numerical solution. The temperature layers and profiles of sample calculations show that it is not acceptable applying the Fourier heat conduction model for estimating the temperature of workpiece. Also, it can be perceived that according to the amount of Vernotte number for a specific Fourier number, it is possible that the temperature of different points of workpiece become even lower than initial temperature.

Keywords: Electrical Discharge Machining (EDM), Non-Fourier Heat Conduction, Numerical Solution, Relaxation Time

Reference: Saedodin, S., Torabi, M. and Eskandar, (2010), H., "Thermal Analysis of Workpiece under Electrical Discharge Machining (EDM), Using Hyperbolic Heat Conduction Model", Int J Advanced Design and Manufacturing Technology, Vol. 3, No. 4, pp. 19-26

Biographical notes: S. Saedodin received his PhD in Mechanical Engineering from Iran University of Science and Technology, Iran. He is currently Assistant Professor at the Department of Mechanical Engineering, Islamic Azad University, Semnan Branch. His current research interest includes heat transfer. **M. Torabi** is graduate student of mechanical engineering, Semnan University. He received his BSc. in solid mechanics from the Azad University of Tehran, Iran. His current research focuses on analytical and computational analysis of heat transfer, microscale heat transfer, non-Fourier conduction heat transfer and ultrafast heat transfer. **H. Eskandar** is graduate student of Mechanical Engineering, Semnan University. He received his BSc. in solid mechanics from the Azad University of Tehran, Iran. His current research focuses on new optimization methods such as imperialist competitive algorithm, discrete optimization, fuzzy control systems and numerical heat transfer.

© 2010 IAU, Majlesi Branch

1 INTRODUCTION

Shaping of materials for modern manufacturing industries with stringent design requirements, such as high precision, complex shapes, and high surface quality, is inevitable to put them in use [1]. To achieve these objectives, advanced machining processes are required [2]. Advanced machining techniques have been classified into four types [2]: mechanical, thermal, chemical machining and electro chemical machining, and biochemical machining processes. Among these, electrical discharge machining (EDM) is a thermal process which has been widely used to produce dies and molds [3]. This high technology is developed in the late 1940s [4], which support about 7% of all machine tool sales in the world [5]. Its unique feature of using thermal energy to machine electrically conductive parts regardless of hardness has been its distinctive advantage in the manufacture of mold, die, automotive, aerospace and surgical components [6]. However, it suffers from few limitations such as low machining efficiency and poor surface finish [7]. To overcome these limitations, a number of efforts have been made to develop such EDM systems that have capability of high material removal rate (MRR), high efficiency, high accuracy and precision without making any major alterations in its basic principle [8-13].

Its method is defined as removing materials from a part by means of a series of repeated electrical discharges between tool called the electrode and the workpiece in the presence of a dielectric fluid [14]. Dielectric fluid acts as an electrical insulation barrier in the gap between the workpiece and electrode. The maximum heat q_0 entering the workpiece due to EDM spark is represented by [15]:

$$q_0 = \frac{4.56 F_c VI}{\pi r_1^{\,2}} \tag{1}$$

Where F_c is the fraction of total EDM spark power going to the cathode, V is the discharge voltage, I is the discharge current and r_1 is the spark radius at the workpiece surface.

It can be perceived from simple calculation that, the heat flux entering the workpiece in EDM process can be more than $10^{11}\, wm^{-2}$. So, if we want to predict the temperature of workpiece during the EMD process, Fourier heat conduction model cannot be applied [16].

In order to eliminate these fails, Cattaneo [17] and Vernotte [18], independently proposed a modification of Fourier's law. This law is now well known as Cattaneo-Vernotte's constitutive equation:

$$\mathrm{q} + \tau \frac{\partial \mathrm{q}}{\partial \mathrm{t}} = -\mathrm{k}\nabla \mathrm{T} \tag{2}$$

Where $\mathbf{q}$ is the heat flux vector, τ is the thermal relaxation time, k is the constant thermal conductivity of the material and ∇T is the temperature gradient. If Eq. (2), combined with the conservation of energy gives the hyperbolic heat conduction equation (HHCE):

$$\frac{\partial T}{\partial t} + \tau \frac{\partial^2 T}{\partial t^2} = \alpha \Delta T \tag{3}$$

Where $\alpha = \dfrac{k}{\rho c}$, ρ, c and Δ are thermal diffusivity, mass density, specific heat capacity and Laplace's differential operator, respectively. Equation (3) is a hyperbolic partial differential equation and causes the propagation speed, reach a limit amount $\sqrt{\alpha/\tau}$, in $\tau > 0$.

There are a lot of literatures that applied HHCE numerically. Chen and Lin [19] applied a hybrid numerical technique to problem in one spatial dimension. Chen [20] combined the Laplace transform, weighting function scheme and the hyperbolic equation, with a conservation term. Zhou et al. [21] presented a thermal wave model of bioheat transfer, together with a seven-flux model, for light propagation and a rate process equation for tissue damage. Yang [22] applied a forward difference method to solved two-dimensional HHCE. Also, he proved the stable condition for the problem. Saedodin et al. [23] investigated a new analytical and numerical technique to calculate temperature field for a cylinder by using hyperbolic model. A review of the literature indicates that there have been no theoretical approaches for applying non-Fourier heat conduction model in EDM process. In the present paper, an effort has been made to study the numerical expression of temperature field is obtained for a cylindrical workpiece in EDM process. Both non-Fourier and Fourier heat conduction equations have been applied for the cylinder. Using our numerical solution, we performed sample calculation of temperature surfaces and profiles for workpiece.

2 PROBLEM STATEMENT

Due to the random and complex nature of EDM, the following assumptions are made to make the problem mathematically tractable.

2.1. Assumptions

1. The domain is considered as axisymmetric.
2. The workpiece material is homogeneous and isotropic.
3. The material properties of the workpiece are temperature independent.
4. The heat transfer to the workpiece is by conduction.

© 2010 IAU, Majlesi Branch

2.2. Thermal model

Consider a cylinder, as shown as Fig. 1. The heat flux due to EDM spark is applied normally to the upper surface ($Z = L$) of the cylinder but only for $r < r_1$.

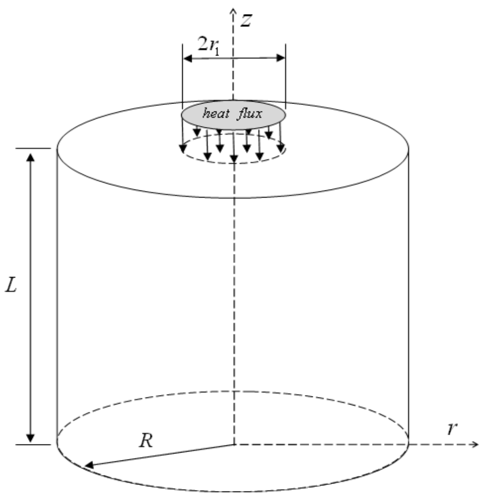

Fig. 1 The cylinder configuration

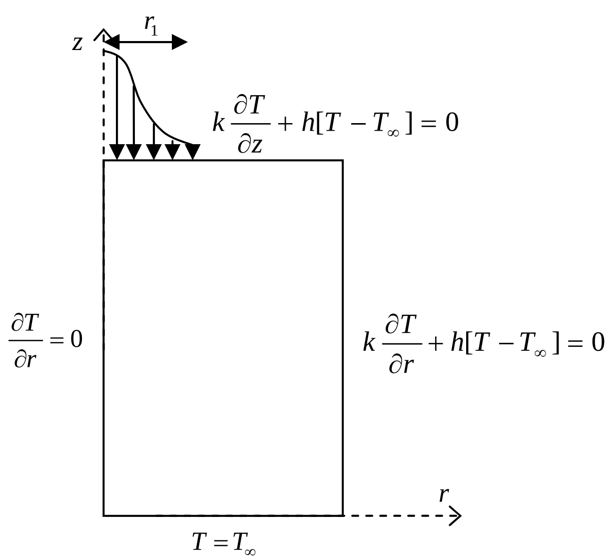

Fig. 2 Thermal model of EDM.

Some researchers [24-26] have considered uniformly distributed heat source within a spark. This assumption is far from reality. This fact is evidenced from the actual shape of a crater formed during EDM. In the present work, a Gaussian heat flux distribution [27, 28] is assumed. If the maximum intensity at the axis of a spark and its radius are known, then the heat flux $q(r)$ at radius r is given by:

$$q(r) = q_0 \exp\{-4.5(\frac{r}{r_1})^2\} \tag{4}$$

2.2.1. Governing differential equation

For this case, the non-Fourier heat conduction equation without any heat generation, the governing equation can then be expressed as:

$$\frac{1}{\alpha}\frac{\partial T}{\partial t} + \frac{\tau}{\alpha}\frac{\partial^2 T}{\partial t^2} = \frac{\partial^2 T}{\partial r^2} + \frac{1}{r}\frac{\partial T}{\partial r} + \frac{\partial^2 T}{\partial z^2} \tag{5}$$

2.2.2. Boundary conditions

Consider the base $(Z = 0)$ surface has been at temperature of dielectric fluid. For this case the boundary conditions are:

$$\frac{\partial T}{\partial r}(0, z, t) = 0 \tag{6a}$$

$$k\frac{\partial T}{\partial r}(R, z, t) + h[T(R, z, t) - T_\infty] = 0 \tag{6b}$$

$$T(r, 0, t) = T_\infty \tag{6c}$$

$$k\frac{\partial T}{\partial z}(r, L, t) =$$

$$\begin{cases} \left.\begin{matrix} q(r) & r < r_1 \\ -h[T(r, L, t) - T_\infty] & r > r_1 \end{matrix}\right\} & for \quad on-ti \\ 0 & for \quad off-ti \end{cases} \tag{6d}$$

2.2.3. Initial conditions

Consider the solid initially has been at the temperature of dielectric fluid. Then:

$$T_i = T_\infty \tag{7}$$

Hence the initial conditions are:

$$T(r, z, 0) = T_\infty \tag{8a}$$

$$\frac{\partial T}{\partial t}(r, z, 0) = 0 \tag{8b}$$

2.3. Normalization

For convenience of subsequent analysis, we introduce the following dimensionless quantities:

$$\theta = k\frac{T - T_\infty}{Lq}, \quad \xi = \frac{r}{R}, \quad \omega = \frac{z}{L}, \quad Fo = \frac{\alpha t}{L^2}$$

$$Ve = \sqrt{\frac{\alpha\tau}{L^2}}, \quad M = (\frac{L}{R})^2 \quad \xi_1 = \frac{r_1}{R} \quad Bi = \frac{hR}{k} \tag{9}$$

Where θ is dimensionless temperature and ξ, ω are dimensionless coordinates. Fo is the Fourier number, Ve is the Vernotte number, M is Square ratio of height to radius of cylinder, ξ_1 is dimensionless radius of heat flux and Bi is the Biot number. By introducing the dimensionless quantities, the normalized temperature of the cylinder obeys the Eq. (10):

© 2010 IAU, Majlesi Branch

$$Ve^2\frac{\partial^2\theta}{\partial Fo^2}+\frac{\partial\theta}{\partial Fo}=M\frac{\partial^2\theta}{\partial\xi^2}+\frac{M}{\xi}\frac{\partial\theta}{\partial\xi}+\frac{\partial^2\theta}{\partial\omega^2} \tag{10}$$

Also, the boundary conditions are:

$$\frac{\partial\theta}{\partial\xi}(0,\omega,Fo)=0 \tag{11a}$$

$$\frac{\partial\theta}{\partial\xi}(1,\omega,Fo)+Bi\,\theta(1,\omega,Fo)=0 \tag{11b}$$

$$\theta(\xi,0,Fo)=0 \tag{11c}$$

$$\frac{\partial\theta}{\partial\omega}(\xi,1,Fo)= \begin{cases} \left.\begin{matrix}\exp\{-4.5(\frac{r}{r_1})^2\} & \xi\le\xi_1 \\ -Bi\,\theta(\xi,1,Fo) & \xi>\xi_1\end{matrix}\right\} & for\quad on-time \\ 0 & for\quad off-time\end{cases} \tag{11d}$$

and the initial conditions are:

$$\frac{\partial\theta}{\partial Fo}(\xi,\omega,0)=0 \tag{12a}$$

$$\theta(\xi,\omega,0)=0 \tag{12b}$$

3 NUMERICAL SOLUTION

To solve this problem numerically, Eq. (10) should be discretized. The discretization can be done in many ways, using Finite Element Method (FEM) or Control Volume Method (CVM). In this work we adopted an implicit Finite Difference Method (FDM). In implicit methods, the finite difference approximations of the individual exact partial derivatives in the partial differential equation are evaluated at the solution time level $n+1$. The implicit schemes are unconditionally stable for any of time step, but the accuracy of the solution is only first-order in time. A forward difference representation is used for time derivative and the central difference representation is used for space derivative. Therefore Eq. (10) can be discretized as the follows:

$$\begin{aligned} &Ve^2\frac{\theta^{n+1}_{i,j}-2\theta^{n}_{i,j}+\theta^{n-1}_{i,j}}{\Delta Fo^2}+\frac{\theta^{n+1}_{i,j}-\theta^{n}_{i,j}}{\Delta Fo}= \\ &M(\frac{\theta^{n+1}_{i+1,j}-2\theta^{n+1}_{i,j}+\theta^{n+1}_{i-1,j}}{\Delta\xi^2}+\frac{\theta^{n+1}_{i+1,j}-\theta^{n+1}_{i-1,j}}{2\xi_{i,j}\Delta\xi}) \\ &+\frac{\theta^{n+1}_{i,j+1}-2\theta^{n+1}_{i,j}+\theta^{n+1}_{i,j-1}}{\Delta\omega^2}\end{aligned} \tag{13}$$

Arranging the Eq. (13) gives:

$$\begin{aligned} &[\frac{Ve^2}{\Delta Fo^2}+\frac{1}{\Delta Fo}+\frac{2M}{\Delta\xi^2}+\frac{2}{\Delta\omega^2}]\theta^{n+1}_{i,j} \\ &+[-\frac{M}{\Delta\xi^2}+\frac{M}{2\xi_{i,j}\Delta\xi}]\theta^{n+1}_{i-1,j}+ \\ &[-\frac{M}{\Delta\xi^2}-\frac{M}{2\xi_{i,j}\Delta\xi}]\theta^{n+1}_{i+1,j} \\ &+\frac{-1}{\Delta\omega^2}(\theta^{n+1}_{i,j+1}+\theta^{n+1}_{i,j-1}) \\ &=[\frac{2Ve^2}{\Delta Fo^2}+\frac{1}{\Delta Fo}]\theta^{n}_{i,j}+[\frac{Ve^2}{\Delta Fo^2}]\theta^{n-1}_{i,j}\end{aligned} \tag{14}$$

In our treatment, we assume $\Delta\xi=\Delta\omega$. Hence, Eq. (14) leads to the following difference equation:

$$\begin{aligned} &[\frac{Ve^2}{\Delta Fo^2}+\frac{1}{\Delta Fo}+\frac{2M}{\Delta\xi^2}+\frac{2}{\Delta\xi^2}]\theta^{n+1}_{i,j}+ \\ &[-\frac{M}{\Delta\xi^2}+\frac{M}{2\xi_{i,j}\Delta\xi}]\theta^{n+1}_{i-1,j}+[-\frac{M}{\Delta\xi^2}-\frac{M}{2\xi_{i,j}\Delta\xi}]\theta^{n+1}_{i+1,j} \\ &+\frac{-1}{\Delta\xi^2}(\theta^{n+1}_{i,j+1}+\theta^{n+1}_{i,j-1})= \\ &[\frac{2Ve^2}{\Delta Fo^2}+\frac{1}{\Delta Fo}]\theta^{n}_{i,j}+[\frac{Ve^2}{\Delta Fo^2}]\theta^{n-1}_{i,j}\end{aligned} \tag{15}$$

The above system of linear algebraic equations can be written in matrix equation as fallowing:

$$[A]\{\theta\}^{n+1}=[B]\{\theta\}^{n}+[C]\{\theta\}^{n-1} \tag{16}$$

Where $[A]$ is five-diagonal matrix, $[B]$ and $[C]$ are just diagonal matrix.

At the center, $\xi=0$, we have $\lim_{\xi\to 0}(\frac{\partial\theta}{\xi\partial\xi})=\frac{\partial^2\theta}{\partial\xi^2}$ by L'Hospital's Rule. Then, Eq. (10) takes the form:

$$Ve^2\frac{\partial^2\theta}{\partial Fo^2}+\frac{\partial\theta}{\partial Fo}=2M\frac{\partial^2\theta}{\partial\xi^2}+\frac{\partial^2\theta}{\partial\omega^2} \tag{17}$$

Hence, Eq. (17) should be discretized for $\xi=0$.

Thanks to inverse method, the dimensionless temperature distribution at each time step can be determined.

As a good comparison, we should solve the same problem with Fourier model. If Fourier's law holds, i.e. in the limit $Ve\to 0$, the Eq. (10) takes the form:

$$\frac{\partial\theta}{\partial Fo}=M\frac{\partial^2\theta}{\partial\xi^2}+\frac{M}{\xi}\frac{\partial\theta}{\partial\xi}+\frac{\partial^2\theta}{\partial\omega^2} \tag{18}$$

The numerical solution corresponds to the mesh size of $\Delta\xi=0.025$ and $\Delta Fo=0.001$

Detailed flow chart of the numerical solution for the cylinder temperature profile is shown in Fig. 3.

© 2010 IAU, Majlesi Branch

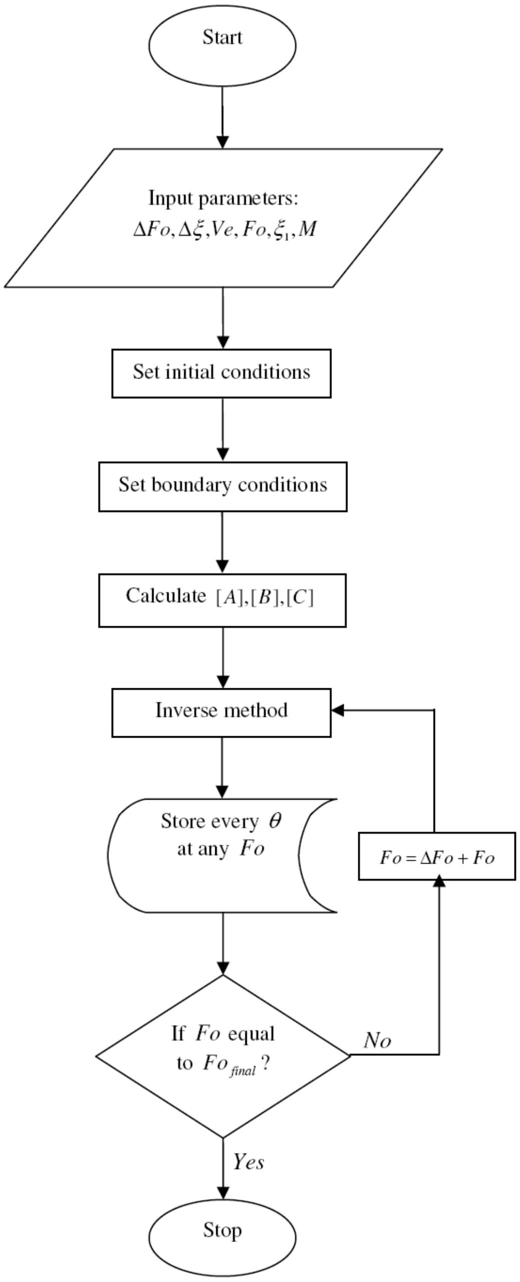

Fig. 3 Flow chart of numerical solution

4 RESULTS AND DISCUSSION

Using our numerical solution, we performed sample temperature surfaces and profiles in the cylinder for the Gaussian type of the heat source. These calculations are obtained for $\xi_1 = 0.2$ and $M = 16$. The results of calculations are presented in Figs. 4-7.

Figures 4 and 5 show the surface temperature profiles for the two cases. It can be perceived from Fig. 4 that, in Fourier model the speed of propagation is infinite. At the moment, all of the workpiece can touch the heat flux. Also, it can be perceived from Fig. 5 that, because of the non-Fourier effect, the heat wave cannot touch the other side of the workpiece at the moment and due to the non-Fourier effects, heat waves can be seen clearly in Fig. 5. As seen in Figs. 4 and 5 the nature of Fourier model and non-Fourier model are completely different and the amount of temperature from these two are not the same. Moreover, these results are in good agreement with another manuscript by Saedodin and Torabi [29].

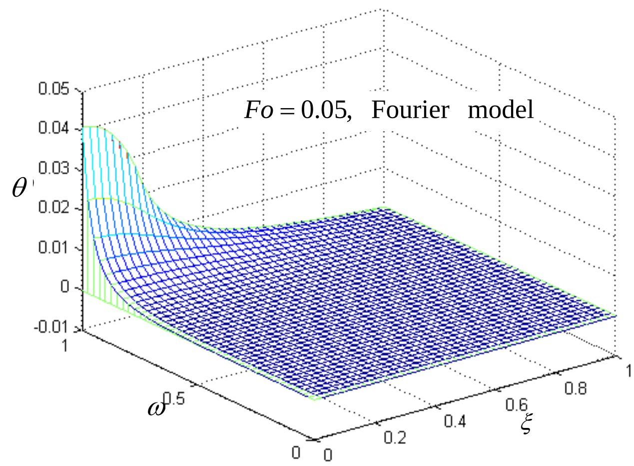

Fig. 4 The surface temperature evolution with $Fo = 0.5$ for Fourier model

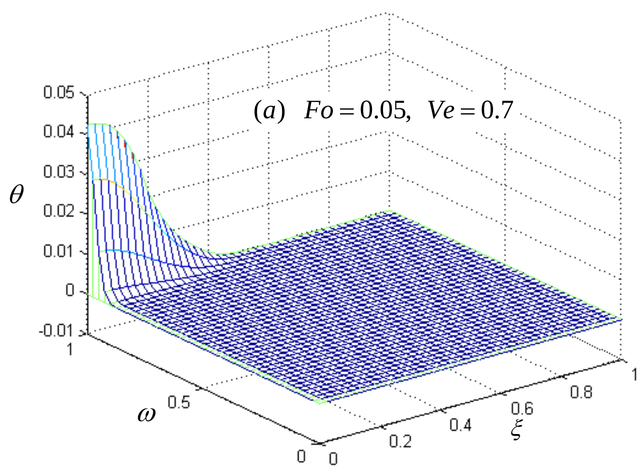

© 2010 IAU, Majlesi Branch

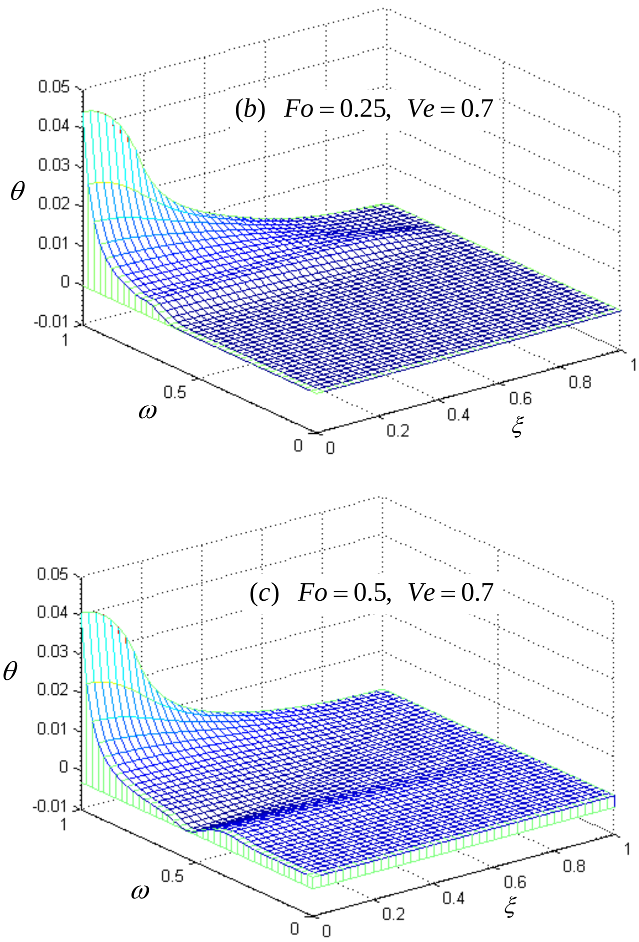

Fig. 5 The surface temperature evolution with $Fo = 0.5$ and $Ve = 0.7$ for non-Fourier model

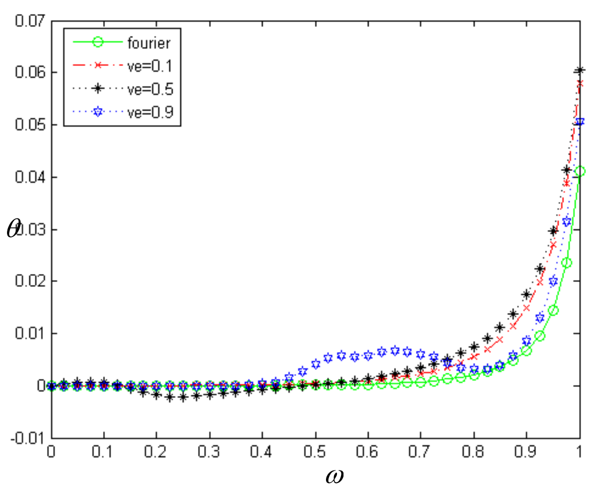

Fig. 6 The temperature distribution for the non-Fourier model with the same Fourier number, but at different Vernotte number along the ω direction

Figure 6 shows temperature profiles along the ω direction at $Fo = 0.5$ and $\xi = 0$ in cylinder. This Fig. shows that, according the amount of Vernotte number for a specific Fourier number, it is possible that the temperature of different points of workpiece become even lower than initial temperature. This interesting behavior does not appear under the Fourier heat conduction model. It is noticeable that, if Fourier model has been applied, the temperature of all points of the workpiece becomes higher than initial temperature. Also, it can be seen that due to the non-Fourier effects, the temperature of lots of points in the workpiece remain steady for some moments.

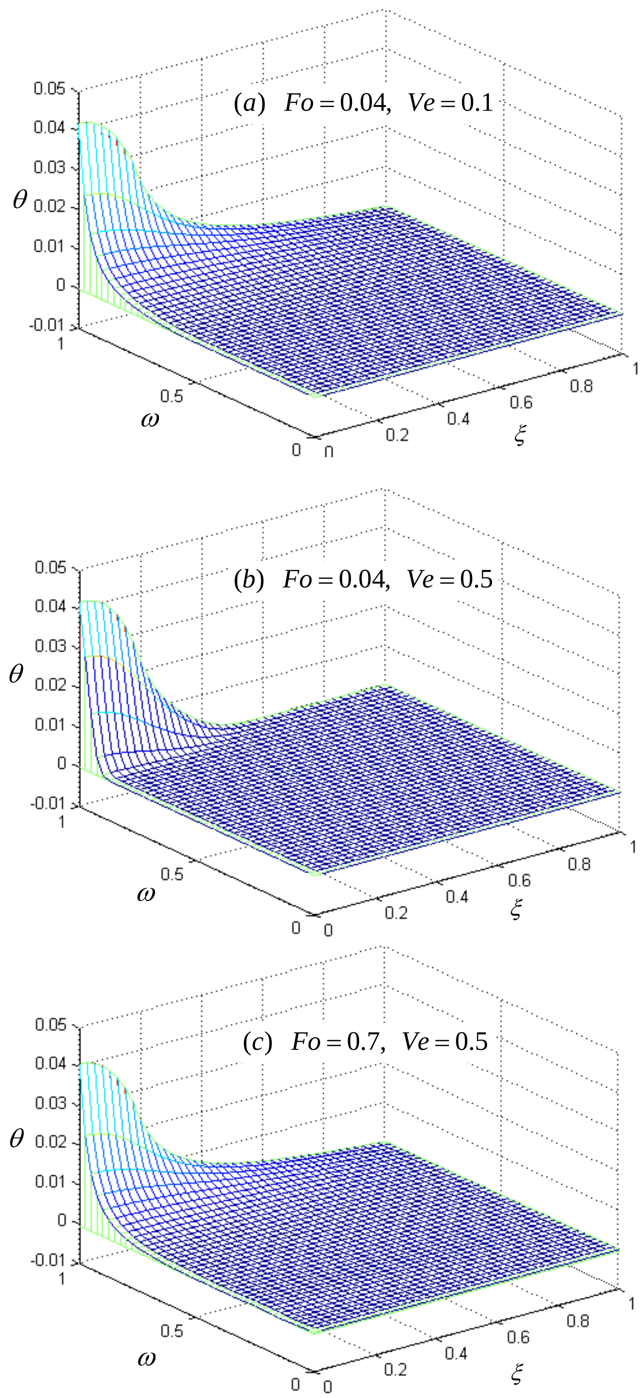

© 2010 IAU, Majlesi Branch

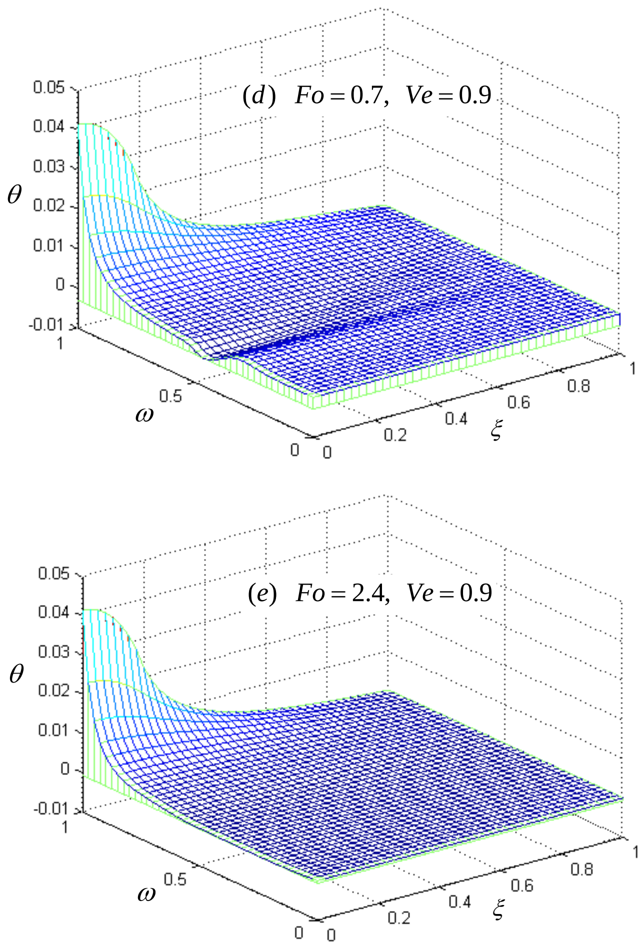

Fig. 7 The surface temperature evolution with different Fourier and Vernotte number

Figure 7 shows surface temperature profiles for the five cases. It can be seen from Fig. 7 that, the higher Vernotte number causes each point to be at initial temperature, more. As it is observed, as much as the Vernotte number increases, the Fourier number that the whole workpiece needs, in order to reach the equilibrium temperature, increases. In addition, it can be deduced from Fig. 7 that, for the same Fourier number as much as the Vernotte number increases, the thermal penetration depth decreases. Regarding Fig. 7, the thermal wave reflection causes the existence of a fracture in the surface temperature profiles of the workpiece. Also, it can be seen that, due to the reflection of heat waves, the temperature of specific points can become lower than initial temperature, especially with $Ve = 0.9$. This interesting behavior does not appear under the Fourier heat conduction model.

5 CONCLUSION

In this paper, the two-dimensional non-Fourier heat conduction model was solved numerically for the cylindrical workpiece in EDM. We concluded that, due to extremely high heat flux during EDM process, calculating the thermal relaxation time is important to predict the temperature of workpiece. Also, it can be seen that, the more the Vernotte number, the more the Fourier number passed for the point that can feel the thermal wave. We also perceived that, the more the Vernotte number, the more the Fourier number needs for the workpiece to reach an equilibrium temperature. Finally, we observed that, applying the Fourier heat conduction model instead of non-Fourier model for predicting the temperature of workpiece during EDM process has significant differences.

REFERENCES

[1] Yadava, V., Jain, V. K., and Dixit, P. M., “Parametric Study of Temperature Distribution in Electrodischarge Diamond Grinding,” Materials and Manufacturing Processes, Vol. 19, 2004, pp. 1071–1101.

[2] Jain, V. K., “Advanced Machining Processes,” Allied Publisher, Bombay, 2001.

[3] Abbas, N. M., Solomon, D. G., and Bahari, M. F., “A Review on Current Research Trends in Electrical Discharge Machining (EDM),” International Journal of Machine Tools and Manufacture, Vol. 47, 2007, pp. 1214–1228.

[4] Singh, S., Maheshwari, S., and Pandey, P. C., “Some Investigations into the Electric Discharge Machining of Hardened Tool Steel using Different Electrode Materials,” Journal of Materials Processing Technology, Vol. 149, 2004, pp. 272–277.

[5] Moser, H., “Growth Industries Rely on EDM,” Manufacturing Engineering, Vol. 127, 2001, pp. 62–68.

[6] Ho, K. H., and Newman, S. T., “State of the Art Electrical Discharge Machining (EDM),” International Journal of Machine Tools and Manufacture, Vol. 43, 2003, pp. 1287–1300.

[7] Kansal, H. K., Singhb, S., and Kumar, P., “Numerical Simulation of Powder Mixed Electric Discharge Machining (PMEDM) using Finite Element Method,” Mathematical and Computer Modelling, Vol. 47, 2008, pp. 1217–1237.

[8] Koshy, P., Jain, V. K., and Lal, G. K., “Experimental Investigations into Electrical Discharge Machining with a Rotating Disc Electrode,” Precision Engineering, Vol. 15, 1993, pp. 6–15.

[9] Soni, J. S., and Chakraverti, G., “Machining Characteristics of Titanium with Rotary Electro Discharge Machining,” Wear, Vol. 171, 1994, pp. 51–58.

[10] Yan, B. H., Wang, C. C., Chow, H. M., and Lin, Y. C., “Feasibility Study of Rotary Electrical Discharge Machining with Ball Burnishing for Al2O3/6061Al Composite,” International Journal of Machine Tools and Manufacture, Vol. 40, 2000, pp. 1403–1421.

[11] Zhao, W. S., Meng, Q. G., and Wang, Z. L., “The Application of Research on Powder Mixed EDM in Rough Machining,” Journal of Materials Processing Technology, Vol. 129, 2002, pp. 30–33.

© 2010 IAU, Majlesi Branch

[12] Kao, C. C., Tao, J., and Shih, A. J., “Near Dry Electrical Discharge Machining,” International Journal of Machine Tools and Manufacture, Vol. 47, 2007, pp. 2273–2281.
[13] Wua, K. L., Yanb, B. H., Leea, J., and Dingb, C. G., “Study on the Characteristics of Electrical Discharge Machining using Dielectric with Surfactant,” journal of materials processing technology, Vol. 209, 2009, pp. 3783–3789.
[14] Luis, C. J., Puertas, I., and Villa, G., “Material Removal Rate and Electrode Wear Study on the EDM of Silicon Carbide,” Journal of Materials Processing Technology, 164–165, 2005, pp. 889–896.
[15] Joshi, S. N., and Pande, S. S., “Development of an Intelligent Process Model for EDM,” The International Journal of Advanced Manufacturing Technology, Vol. 45, 2009, pp. 300–317.
[16] Maurer, M. J., and Thompson, H. A., “Non-Fourier Effects at High Heat Flux,” Journal of Heat Transfer, Vol. 95, 1973, pp. 284-286.
[17] Cattaneo, C., “Sur une forme de l’équation de la chaleur éliminant le paradoxe d’une propagation instantanée,” C. R. Acad. Sci., Vol. 247, 1958, pp. 431–433.
[18] Vernotte, P., “Les paradoxes de la théorie continue de l’équation de la chaleur,” C. R. Acad. Sci., Vol. 246, 1958, pp. 3154–3155.
[19] Chen, H. T., and Lin, J. Y., “Numerical Analysis for Hyperbolic Heat Conduction,” International Journal of Heat and Mass Transfer, Vol. 36, 1992, pp. 2891–2898.
[20] Chen, T. M., “Numerical Solution of Hyperbolic Heat Conduction in Thin Surface Layers,” International Journal of Heat and Mass Transfer, Vol. 50, 2007, pp. 4424–4429.
[21] Zhou, J., Zhang, Y., and Chen, J. K., “Non-Fourier Heat Conduction Effect on Laser-Induced Thermal Damage in Biological Tissues,” Numerical Heat Transfer, Part A, Vol. 54, 2008, pp. 1–19.
[22] Yang, C. Y., “Direct and Inverse Solutions of the Two-Dimensional Hyperbolic Heat Conduction Problems,” Applied Mathematical Modelling, Vol. 33, 2009, pp. 2907–2918.
[23] Saedodin, S., Torabi, M., Eskandar, H., and Akbari, M., “Analytical and Numerical Solution of Non-Fourier Heat Conduction in Cylindrical Coordinates,” Journal of Computational Analysis and Applications (to be published)
[24] Jilani, S. T., and Pandey, P. C., “Analysis and Modeling of EDM Parameters,” Precision Engineering, Vol. 4, 1982, pp. 215–221.
[25] DiBitonto, D. D., Eubank, P. T., Patel, M. R., and Barrufet, A., “Theoretical Models of the Electrical Discharge Machining Process—I: a Simple Cathode Erosion Model,” Journal of Applied Physics, Vol. 66, 1989, pp. 4095–4103.
[26] Patel, M. R., Barrufet, A., Eubank, P. T., and DiBitonto, D.D., “Theoretical Models of the Electrical Discharge Machining Process—II: the Anode Erosion Model,” Journal of Applied Physics, Vol. 66, 1989, pp. 4104–4111.
[27] Madhu, P., Jain, V. K., Sundarajan, T., and Rajurkar, K. P., “Finite Element Analysis of EDM Process,” Processing of Advanced Materials, Vol. 1, 1991, pp. 161–173.
[28] Yadav, V., Jain, V. K., and Dixit, P. M., “Thermal Stresses Due to Electrical Discharge Machining,” International Journal of Machine Tools and Manufacture, Vol. 42, 2002, pp. 877–888.
[29] Saedodin S. and Torabi M., “Electrical Discharge Machining (EDM) by Using Non-Fourier Heat Conduction Model,” Contemporary Engineering Sciences, Vol. 3, 2010, pp. 269-283

© 2010 IAU, Majlesi Branch